PHYSICAL REVIEW A VOLUME 43, NUMBER 11 1 JUNE 1991

Quantum nondemolition measurements using a fully quantized parametric interaction

M. J. Gagen and G. J. Milburn
Department of Physics, The University of Queensland, QLD 4072, Australia
(Received 11 July 1990; revised manuscript received 28 December 1990)

A quantum nondemolition measurement based on a three-mode interaction mediated by a second-order nonlinear susceptibility is discussed. All three modes are treated quantum mechanically. The signal field is taken as one of the three modes and the probe field is the combined field in the other two modes. If the probe system is initially in a number state, the interaction between the signal and probe is equivalent to that between a harmonic oscillator and an angular momentum system. Photon counting on the probe field realizes a quantum nondemolition measurement of the square of a quadrature phase amplitude of the signal, and thus provides a direct measurement of second-order squeezing.

I. INTRODUCTION

The recent consideration of gravitational radiation detection schemes has generated considerable interest in quantum nondemolition (QND), or back action evading (BAE) schemes. The objective of such schemes is to monitor very weak, or perhaps quantum limited, signals without adding noise to the component of the signal carrying the desired information. Recently, there has been some success in performing quantum nondemolition measurements in the optical regime. La Porta *et al.*[1] and Yurke[2] have used a parametric down-converter to perform a QND measurement of the optical quadrature of a signal mode. Bachor *et al.*[3] have demonstrated the feasibility of QND measurements in an optical-fiber ring resonator. BAE techniques have also been suggested as a means to generate superpositions of macroscopically separated coherent states using the parametric conversion process.[4] These results complement those obtained using four-wave mixing in optical fibers[5] and similar schemes to generate macroscopically distinguishable coherent states.[6–8]

The BAE measurements using parametric down-conversion employ three-mode systems consisting of a signal mode, a readout mode, and a strong, classical, nondepleted coherent pump. Of interest is the case where we fully quantize the pump field, as we can then consider pump-field states other than coherent states.

The natural way to fully quantize a three-mode system is to treat as separate the signal mode interacting with a two-mode probe. It is then possible to treat the two-mode probe as a single quantum system. In fact we will show that the probe may be treated as a spin system, using the boson representation of angular momentum.[9–11] This formalism simplifies a three-mode problem to the conceptually simpler problem of the harmonic oscillator coupled to an angular momentum system.

The usual quantum treatment of three modes treats one of the modes, the pump, as being in a classical, nondepleted coherent state. In this case, the parametric interactions being considered simplify to an interaction between a signal and a one-mode probe field. It is systems similar to these that are used to generate the normal BAE measurements discussed in Refs. 1 and 2. It is of interest to us to pump the crystal with a nonclassical pump. Using photon-number states, the two-mode probe system may be transformed to an angular momentum system with a total angular momentum equal to half the total photon number in the two modes. As we will show, the QND gain is controlled by this number. It may be possible to prepare such a probe state using feedback-generated sub-Poissonian light.[12,13]

There are two feedback schemes which might be appropriate. The first scheme takes the phase-reversed photo current output from a photodetector and adds this current to the dc bias current of the diode laser illuminating the detector.[12] The usefulness of such a scheme depends on the availability of a source appropriate for a parametric interaction. A second, more versatile, scheme involves placing an optoelectronic beam splitter between a laser source and a photodetector and driving the beam splitter with the output current of the photodetector in such a way that the transmittivity decreases if the current increases. Such a scheme has been analyzed in some detail by Shapiro *et al.*[14]

A variant of this scheme that reduces the photon-number fluctuations in a single cavity mode would use the current-driven beam splitter as the output from an optical cavity driven by an intense coherent field.[15] This latter scheme is probably the most appropriate for the application considered in this paper, and is indicated schematically in Fig. 1.

We consider the ideal case in which one mode of the two-mode probe is prepared in a number state, with a very large photon-number occupancy (see Fig. 1). The other mode of the probe is initially prepared in the vacuum state. The total probe photon number is conserved and the probe-signal interaction will simply rotate the angular momentum vector which describes the probe state. It is the detection of this rotation that enables us to perform BAE measurements on the signal mode. This may be achieved by photon counting on one of the probe

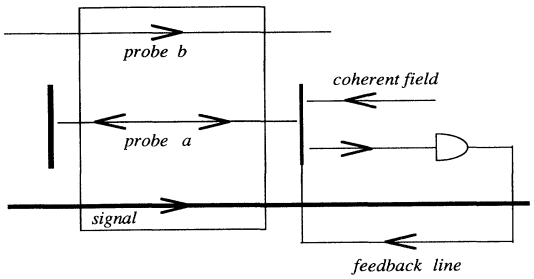

FIG. 1. Schematic outline of our three-mode system. The signal mode (c) is in some arbitrary initial state. The b mode is prepared in a vacuum state. The a mode is in a feedback-generated sub-Poissonian state and ideally will be the number state $|N\rangle_a$ with large N. The a and b modes together form a two-mode probe. The probe-signal system interacts via a parametric interaction $\hat{H}=\hbar\chi\hat{J}_x\hat{X}_c$. Subsequent photon detection performed on the b mode will condition the signal mode into a near eigenstate of $\cos(\kappa\hat{X}_c)$.

modes at the output. We expect the reduced noise properties of this ideal number state pump to give an improved signal-to-noise ratio for the BAE measurement of a quadrature component of the signal mode.

Song and Caves[5] have suggested the use of a parametric down-converter driven by a coherent pump to generate superpositions of two macroscopically distinguishable coherent states. In our model with a fully quantized treatment and the pump field prepared in a number state, multiple superpositions of coherent or squeezed states in the signal mode may be prepared.

In Sec. II we first specify our three-mode Hamiltonian and the SU(2) notation for the two-mode probe. The Heisenberg equations of motion permit a heuristic understanding of the BAE measurement and the resulting signal-mode superposition of squeezed states. In Sec. III we obtain the signal-to-noise ratio (SNR) and show that for this system, conditional photon counting is equivalent to a measurement of second-order squeezing. We also employ some additional correlation functions to investigate the quality of our QND measurement scheme. In Sec. IV we discuss photon counting in one of the modes of the probe and show that this is equivalent to a determination of the angular momentum of the two-mode probe. We then condition the signal mode based on the result of the photon count. In Sec. V we explore the effect of nonunit quantum photon detection efficency for the system of interest. Throughout the paper the response of the system to a general squeezed state input signal is determined and the conditional probability distributions of the desired quadrature component of the signal are plotted.

II. TWO-MODE SPIN HAMILTONIAN

We seek to model the interaction of three fully quantized electromagnetic modes with annihilation operators a, b, and c. Two of these modes, a and b, form our probe spin system and the third, c, is the signal mode upon which QND measurements are performed. The quadrature components are defined for each mode as

$$\hat{X}_\alpha=\tfrac{1}{2}(\alpha+\alpha^\dagger)\ , \tag{2.1a}$$

$$\hat{Y}_\alpha=\frac{-i}{2}(\alpha-\alpha^\dagger)\ , \tag{2.1b}$$

where α designates the operators a, b, or c.

The Hamiltonian for three modes interacting via a second-order nonlinearity may be written two ways, depending on the frequency relationships of the fields,

$$\hat{H}_+=\hbar\frac{\chi_+}{2}(a^\dagger bc+ab^\dagger c^\dagger)\ , \tag{2.2a}$$

$$\hat{H}_-=\hbar\frac{\chi_-}{2}(a^\dagger bc^\dagger+ab^\dagger c)\ , \tag{2.2b}$$

where $\chi_\pm$ is proportional to the second-order nonlinearity. For $\hat{H}_+$ we require $\omega_a-\omega_b=\omega_c$ and for $\hat{H}_-$ we require $\omega_b-\omega_a=\omega_c$. If a is regarded as the annihilation operator for the pump mode, $\hat{H}_+$ describes nondegenerate parametric amplification while $\hat{H}_-$ describes frequency conversion.

One way to treat the fully quantized probe, (modes a and b), is by introducing the Hermitian operators.[9,10]

$$\hat{J}_x=\tfrac{1}{2}(a^\dagger b+ab^\dagger)\ , \tag{2.3a}$$

$$\hat{J}_y=\frac{-i}{2}(a^\dagger b-ab^\dagger)\ , \tag{2.3b}$$

$$\hat{J}_z=\tfrac{1}{2}(a^\dagger a-b^\dagger b)\ , \tag{2.3c}$$

and the total probe photon number is

$$\hat{N}=a^\dagger a+b^\dagger b\ . \tag{2.4}$$

These operators (Eq. 2.3) satisfy the usual SU(2) Lie algebra of

$$[\hat{J}_x,\hat{J}_y]=i\hat{J}_z\ , \tag{2.5}$$

together with cyclic permutations of x, y, and z. The Casimir invariant for this group is

$$\hat{J}^2=\frac{\hat{N}}{2}\left[\frac{\hat{N}}{2}+1\right]\ . \tag{2.6}$$

As $\hat{J}^2$ is invariant and depends only on $\hat{N}$, then any system Hamiltonian commuting with $\hat{J}^2$ will conserve $\hat{N}$. This will be satisfied in our case.

Using these operators gives insight into the structure of $\hat{H}_+$ and $\hat{H}_-$. We have

$$\hat{H}_\pm=\hbar\chi_\pm(\hat{J}_x\hat{X}_c\mp\hat{J}_y\hat{Y}_c)\ . \tag{2.7}$$

Here we see that these three-mode Hamiltonians obviously commute with $\hat{J}^2$, and hence always conserve the probe photon number $\hat{N}$. We model our QND system by an effective Hamiltonian,

$$\begin{aligned}\hat{H}&=\tfrac{1}{2}(\hat{H}_++\hat{H}_-)\\&=\hbar(\chi\hat{J}_x\hat{X}_c-\Gamma\hat{J}_y\hat{Y}_c)\ ,\end{aligned} \tag{2.8}$$

where we have defined the average value of second-order nonlinearities and their difference as

$$\chi=\tfrac{1}{2}(\chi_+ +\chi_-)\ , \tag{2.9a}$$

$$\Gamma=\tfrac{1}{2}(\chi_+ -\chi_-)\ . \tag{2.9b}$$

For the case where $\Gamma=0$, we are in a position to be able to model QND detection of $\hat{X}_c$ via measurements of the probe operator conjugate to $\hat{J}_x$, namely, $\hat{J}_z$.

Some insight into the system with $\Gamma=0$ can be gained if mode a were treated as a classical nondepleted pump: The total Hamiltonian in Eq. (2.8) ($\Gamma=0$) would be proportional to $\hat{X}_b\hat{X}_c$. This would enable a QND measurement of the signal quadrature $\hat{X}_c$ to be made by monitoring the probe quadrature $\hat{Y}_b$. Such a scheme has indeed been implemented by La Porta *et al.*[1,2]

This measurement of $\hat{J}_z$ is equivalent to measuring $\hat{n}_b=b^\dagger b$, the b-mode photon number operator. This can be seen as follows: We prepare the probe in an eigenstate of $\hat{N}$ which commutes with $\hat{J}^2$ and is thus conserved. Given such a state for modes a and b and a knowledge of $\hat{N}$, we only need measure either $\hat{n}_a=a^\dagger a$ or $\hat{n}_b=b^\dagger b$ to effect a measurement of $\hat{J}_z$. We will consider $\hat{n}_b$ measurements.

An equivalent conditioning measurement is used in Ref. 5. Here a classical, nondepleted coherent pump is used with a two-mode Hamiltonian $\hat{H}\approx\hat{X}_b\hat{X}_c$. The QND measurement is effected by photon counting on the b-mode probe, and serves to condition the c-mode signal into near eigenstates of $\hat{X}_c$.

The Heisenberg equations of motion for the probe are

$$\frac{d}{dt}\begin{bmatrix}\hat{J}_x\\ \hat{J}_y\\ \hat{J}_z\\ \hat{X}_c\\ \hat{Y}_c\end{bmatrix}=\begin{bmatrix}-\Gamma\hat{J}_z\hat{Y}_c\\ -\chi\hat{J}_z\hat{X}_c\\ \chi\hat{J}_y\hat{X}_c+\Gamma\hat{J}_x\hat{Y}_c\\ -\frac{1}{2}\Gamma\hat{J}_y\\ -\frac{1}{2}\chi\hat{J}_x\end{bmatrix}\ . \tag{2.10}$$

We are interested in a measurement of $\hat{J}_z$, and therefore have to solve a nonlinear system for $\Gamma\neq0$. The dependence of $\hat{J}_z$ in terms of signal-mode operators can be obtained by noting

$$\frac{d}{dt}(\hat{J}_z)=-\frac{d}{dt}\left[\frac{\chi}{\Gamma}\hat{X}_c^{\,2}+\frac{\Gamma}{\chi}\hat{Y}_c^{\,2}\right] \tag{2.11}$$

for $\chi,\Gamma\neq0$ and hence

$$\hat{J}_z(t)=\hat{J}_z(0)-\frac{\chi}{\Gamma}[\hat{X}_c^{\,2}(t)-\hat{X}_c^{\,2}(0)]-\frac{\Gamma}{\chi}[\hat{Y}_c^{\,2}(t)-\hat{Y}_c^{\,2}(0)]\ , \tag{2.12a}$$

$$\hat{n}_b(t)=\frac{\chi}{\Gamma}[\hat{X}_c^{\,2}(t)-\hat{X}_c^{\,2}(0)]+\frac{\Gamma}{\chi}[\hat{Y}_c^{\,2}(t)-\hat{Y}_c^{\,2}(0)]+\hat{n}_b(0)\ . \tag{2.12b}$$

These solutions display the expected (and known) behavior for $\chi=\pm\Gamma$, where we have, respectively,

$$\hat{n}_b(t)=\pm[n_c(t)-n_c(0)]+\hat{n}_b(0)\ . \tag{2.13}$$

For the case $\chi=\Gamma$ we have that $H=H_+\sim a^\dagger bc+ab^\dagger c^\dagger$ and expect that $n_b(t)-n_c(t)=$const as the b- and c-mode photons are created and destroyed in pairs. For the case where $\chi=-\Gamma$ we have $H=H_-\sim a^\dagger bc^\dagger+ab^\dagger c$ and expect that $n_b(t)+n_c(t)=$const as photons are exchanged between the b and c modes.

We are interested in the case where $\chi_+\approx\chi_-$ and $\Gamma\approx0$. In this regime we see that

$$J_z(t)=-\frac{\chi}{\Gamma}[\hat{X}_c^{\,2}(t)-\hat{X}_c^{\,2}(0)]\ . \tag{2.14}$$

The interesting feature displayed here is that for small Γ, we expect a measurement of $\hat{J}_z$ to condition the signal mode into near eigenstates of $\hat{X}_c(t)$. This same feature was found in Ref. 5.

For the case of $\Gamma=0$, the Heisenberg equations of motion decouple and are solvable. We consider this case for the rest of this paper, and the Heisenberg equations of motion become

$$\frac{d}{dt}\begin{bmatrix}\hat{J}_x\\ J_y\\ \hat{J}_z\end{bmatrix}=\begin{bmatrix}0&0&0\\ 0&0&-\chi\hat{X}_c\\ 0&\chi\hat{X}_c&0\end{bmatrix}\begin{bmatrix}\hat{J}_x\\ \hat{J}_y\\ \hat{J}_z\end{bmatrix}\ . \tag{2.15}$$

When $\Gamma=0$, we have that $(d/dt)(\hat{X}_c)=0$ and therefore $\hat{X}_c$ is a constant of motion. Noting this, the solution to Eq. 2.15 is

$$\hat{J}_x(t)=\hat{J}_x(0)\ , \tag{2.16a}$$

$$\hat{J}_y(t)=\cos(\chi t\hat{X}_c)\hat{J}_y(0)-\sin(\chi t\hat{X}_c)\hat{J}_z(0)\ , \tag{2.16b}$$

$$\hat{J}_z(t)=\sin(\chi t\hat{X}_c)\hat{J}_y(0)+\cos(\chi t\hat{X}_c)\hat{J}_z(0)\ . \tag{2.16c}$$

Here we see the expected rotation of the probe operators depending on the strength of the interaction χt and the $\hat{X}_c$ quadrature component of the signal field.

The eigenstates of $\hat{J}_z$ are $|j,j-m\rangle$ where $j=N/2$ and $m=0,1,2,\ldots,2j$. In terms of the number states of modes a and b this is

$$|j,j-m\rangle\equiv|2j-m\rangle_a\otimes|m\rangle_b\ . \tag{2.17}$$

As stated above, we prepare the probe in an eigenstate of N, and have the initial state

$$|\psi_{\rm in}\rangle=|j,j\rangle\equiv|N\rangle_a\otimes|0\rangle_b\ . \tag{2.18}$$

Then the expectation value of $\hat{J}_z(t)$ will be

$$\langle\hat{J}_z(t)\rangle=j\langle\cos(\chi t\hat{X}_c)\rangle\ . \tag{2.19}$$

Therefore, we expect that a readout of $\hat{J}_z$ at time t will yield information on the $\hat{X}_c$ quadrature component as previously indicated for the case $\Gamma\approx0$. (This is a little like the number measurements using $a^\dagger ab^\dagger b$ discussed in Milburn and Walls.[16]) Indeed, as $\cos(\chi t\hat{X}_c)$ is a multivalued function, a readout of $\hat{J}_z$ must force the signal mode c into a superposition of near eigenstates of $\hat{X}_c$. (A similar superposition of states is obtained in Ref. 5 where a classical nondepleted pump was used to generate a su-

perposition of two macroscopically distinguishable coherent states.)

We expect that the conditional probability distribution function for $\hat{X}_c$ will reflect this superposition of states. We see this in Eq. (2.19) where a readout of m photons in the b mode will condition the c mode into near eigenstates of $\hat{X}_c$ (with eigenvalues x), satisfying the multivalued equation

$$\cos(\chi t x)=\frac{N-2m}{N} . \tag{2.20}$$

We will show that the probability distribution of $\hat{X}_c$ does indeed peak at the expected values of x. When $\chi t \ll 1$ (the usual situation), Eq. (2.20) becomes

$$x^2=\frac{2m}{N(\chi t)^2} . \tag{2.21}$$

In this limit we expect the conditional probability distribution for $\hat{X}_c$, given a result m for the b-mode photon count, to be double peaked at $\pm(2m/N\chi^2 t^2)^{1/2}$.

III. SIGNAL-TO-NOISE RATIO

It is of interest to compare the signal-to-noise ratio (SNR) for this system, consisting of a probe (a two-mode angular momentum system) and signal, with the SNR of a balanced homodyne detector, for instance. Throughout this section we employ the number state pump shown in Eq. (2.18). In a later section we consider pump states with increased photon-number fluctuations. We define the SNR ($\mathcal{S}$) as

$$\mathcal{S}=\frac{\langle \hat{n}_b \rangle}{\langle \Delta \hat{n}_b^{\,2} \rangle^{1/2}} , \tag{3.1}$$

where $\Delta\hat{n}_b=\hat{n}_b-\langle \hat{n}_b \rangle$. Writing $\hat{O}_c=\cos(\kappa\hat{X}_c)$ and $\kappa=\chi t$, this gives

$$\mathcal{S}=\frac{1-\langle \hat{O}_c \rangle}{[(1/N)(1-\langle \hat{O}_c^{\,2} \rangle)+\langle \hat{O}_c^{\,2} \rangle-\langle \hat{O}_c \rangle^2]^{1/2}} . \tag{3.2}$$

It is noted that for large N the first term in the denominator will not contribute, and further for small $\kappa \ll 1$ we can expand to first order, giving

$$\mathcal{S}=\frac{\langle \hat{X}_c^{\,2} \rangle}{\langle (\Delta \hat{X}_c^{\,2})^2 \rangle^{1/2}} . \tag{3.3}$$

We see that in the limit of large N, the signal-to-noise ratio of the probe photon count is equal to the signal-to-noise ratio of the signal operator $\hat{X}_c^{\,2}$, and thus for large N the model permits a QND measurement of this operator. The number N thus plays the role of QND gain. It is interesting to compare $\mathcal{S}$ for $\hat{X}_c^{\,2}$ to that for balanced homodyne detection of $\hat{X}_c$,[17]

$$\mathcal{S}_{\rm BH}=\frac{\langle \hat{X}_c \rangle}{\langle (\Delta \hat{X}_c)^2 \rangle^{1/2}} \tag{3.4}$$

We can compare these two $\mathcal{S}$'s for the case of a coherent input signal. For a coherent state $|\gamma\rangle$ we have an expectation value of $\hat{X}_c$, $\langle \hat{X}_c \rangle=\frac{1}{2}(\gamma+\gamma^*)$. For large $\langle \hat{X}_c \rangle$, the $\mathcal{S}$ of Eq. (3.3) is roughly half the value of that for the balanced homodyne detector. This gives this spin probe system an efficiency (for large $\langle \hat{X}_c \rangle$) roughly comparable to direct photon detection of the c-mode signal.[17]

It is of interest to consider the case when $\langle \hat{X}_c \rangle \approx 0$. Then we have that $\mathcal{S}_{\rm BH} \to 0$ reflecting the loss of the received signal. However, we have that $\mathcal{S} \to 2^{-1/2}$ for $\langle \hat{X}_c \rangle \approx 0$. This is because a measure of $\hat{X}_c^{\,2}$ when $\langle \hat{X}_c \rangle = 0$ is a measure of the quadrature noise in the signal mode. In a vacuum coherent state, $\langle \hat{X}_c^{\,2} \rangle = \frac{1}{4}$ and $\langle (\Delta \hat{X}_c^{\,2}) \rangle^{1/2} = \sqrt{2}/4$, giving a $\mathcal{S}$ of $1/\sqrt{2}$. This same result applies for a general squeezed state when both the signal $\langle \hat{X}_c^{\,2} \rangle$ and the variance $\langle (\Delta \hat{X}_c^{\,2})^2 \rangle$ are squeezed by the same factor.

The dependence of $\mathcal{S}$ on the variance of the square of the $\hat{X}_c$ operator raises the prospect of directly measuring the higher-order squeezing[17,18] of the signal field. Higher-order squeezing is said to occur when the higher moments of the quadrature phase take on values less than their coherent-state values. That is,

$$\langle (\Delta \hat{X}_c)^n \rangle < (n-1)!!(\tfrac{1}{2})^n . \tag{3.5}$$

Here, n is restricted to be even since the above condition is uniquely nonclassical for the even moments.

As Hong and Mandel[19] point out, higher-order squeezing might give particular benefits from the point of view of noise reduction, because the higher-order moments ($n>2$) suffer a larger fractional reduction. This is exactly what we have seen, with a significantly enhanced SNR in the small $\langle \hat{X}_c \rangle$ regime.

Recently, a number of quantities have been proposed as a measure of the quality of a QND measurement.[20] The first of these quantities determines the degree of correlation between the probe readout and the signal QND variable $\hat{O}_c=\cos(\kappa\hat{X}_c)$,

$$C^2(\hat{O}_c^{\,\rm in},\hat{J}_z^{\,\rm out})=\frac{|\langle \hat{O}_c^{\,\rm in}\hat{J}_z^{\,\rm out} \rangle-\langle \hat{O}_c^{\,\rm in} \rangle\langle \hat{J}_z^{\,\rm out} \rangle|^2}{V(\hat{O}_c^{\,\rm in})V(\hat{J}_z^{\,\rm out})}$$

$$=\frac{V(\hat{O}_c^{\,\rm in})}{\frac{1}{N}\langle \hat{O}_s^{\,2} \rangle+V(\hat{O}_c^{\,\rm in})} , \tag{3.6}$$

where we write $\hat{O}_s=\sin(\kappa\hat{X}_c)$, and $V(\hat{O}_c^{\,\rm in})$ is the variance of $\hat{O}_c^{\,\rm in}$ for the initial state. For a perfect measurement device the correlation coefficient is unity, and this is achieved in the case where N becomes large. There are a further two correlation coefficients of interest. The first is a measure of the correlation between the signal input field, and the signal output field, $C^2(\hat{O}_c^{\,\rm in},\hat{O}_c^{\,\rm out})$, and is equal to one as is expected for a perfect QND measurement. The second provides an indication of how good the system is as a signal-mode state preparation device. The signal mode is conditioned into eigenstates of $\hat{O}_c=\cos(\kappa\hat{X}_c)$ and so we would expect the variance of this quantity, conditioned on the probe readout, to be zero for a good QND measurement. In fact, we have $V(\hat{O}_c^{\,\rm out}|\hat{J}_z^{\,\rm out}) \approx 0$ for large N, and the signal-mode output state is indeed in a near eigenstate of $\cos(\kappa\hat{X}_c)$. A near eigenstate of $\cos(\kappa\hat{X}_c)$ is made up of a superposition of

near eigenstates of $\hat{X}_c$ as suggested by our previous heuristic analysis. That this is so is shown by a large variance in $\hat{X}_c$ and we can show that $V(\hat{X}_c^{\text{out}}|\hat{J}_z^{\text{out}})$ is nonzero and has a complicated dependence on the initial signal state.

IV. CONDITIONAL MEASUREMENT

The b-mode photon detection will be performed on the output state $|\psi_{\text{out}}\rangle$. This is obtained by unitarily evolving $|\psi_{\text{in}}\rangle$ under the influence of $\hat{H}$. This unitary evolution is equivalent to a rotation about the $\hat{J}_x$ axis by an amount proportional to the signal quadrature phase amplitude. We have

$$|\psi_{\text{out}}\rangle = e^{-i\kappa\hat{J}_x\hat{X}_c}|\psi_{\text{in}}\rangle = \int_{-\infty}^{\infty} dx\, e^{-i\kappa x\hat{J}_x}|j,j\rangle\otimes|x\rangle\langle x|\phi_c\rangle , \tag{4.1}$$

where we have used a resolution of identity in terms of the eigenstates of $\hat{X}_c$. The c-mode input signal state is written $|\phi_c\rangle$.

The rotation of the two-mode $|jj\rangle$ state is given in terms of the usual rotation matrices.[9,21] We have

$$|\psi_{\text{out}}\rangle = \sum_{m=0}^{N}\int dx\, C_m(\kappa x)\langle x|\phi_c\rangle|j,j-m\rangle\otimes|x\rangle , \tag{4.2}$$

$$C_m(\kappa x) = \begin{bmatrix} N \\ m \end{bmatrix}^{1/2}\left[\cos\left[\frac{\kappa x}{2}\right]\right]^{N-m}\left[i\sin\left[\frac{\kappa x}{2}\right]\right]^{m} \tag{4.3}$$

are the rotation matrix elements depending on the eigenvalues of $\hat{X}_c$.

A photon detection measurement ($\hat{n}_b$) is then performed on the b mode of the probe. Due to the conservation of $\hat{N}$, the total photon number, the measurement of m photons in the b mode serves to project the probe into the state $|j,j-m\rangle$. (Alternatively, if we have a classical nondepleted pump, then $|\psi_{\text{out}}\rangle$ is given by a two-mode unitary evolution generated from the equivalent Hamiltonian $\hat{X}_b\hat{X}_c$. The output state will be a two-mode squeezed state.[22] The conditional measurement of $\hat{n}_b$ will then simply project the b mode into a number state with the usual squeezed-state probability distribution, and, as shown in Ref. 5, this measurement will condition the signal mode into a superposition of squeezed states.)

The conditional measurement of m photons in the b mode would usually be treated using the simple projection operator $|m\rangle_b\langle m|$. While this would be satisfactory for our immediate purposes in calculating the probability distribution of m, we will later be interested in taking the nonunit quantum efficiency of photon detection into account. In addition, photon counting is usually done destructively and, realistically, the counting of m photons in the b mode will generally leave the b mode in the vacuum state. We can easily take these effects into account using the effects and operations formalism of measurement theory.[23–25]

The selective measurement of m photons in the b mode can be described by an operation $\tilde{\phi}$ on the original density matrix $\hat{\rho}$, giving

$$\hat{\rho}^m = \tilde{\phi}\hat{\rho}/\text{tr}(\tilde{\phi}\hat{\rho}) = \hat{\Gamma}_\eta(m)\hat{\rho}\hat{\Gamma}_\eta^\dagger(m)/\text{tr}(\tilde{\phi}\hat{\rho}) , \tag{4.4}$$

where $\hat{\Gamma}_\eta(m)$ takes account of the nonunit quantum efficiency of photon detection, $\eta\le 1$, and whether the measurement is destructive or not. For a QND, or nondestructive counting of photons, we have

$$\hat{\Gamma}_\eta^{\text{QND}}(m) = \sum_{k=m}^{\infty}\left[\begin{bmatrix} k \\ m \end{bmatrix}\eta^m(1-\eta)^{k-m}\right]^{1/2}|k\rangle_b\langle k| . \tag{4.5}$$

It is evident that for $\eta=1$, $\Gamma\to|m\rangle\langle m|$, which gives the usual nondestructive projection operator. Equation (4.5) has an obvious interpretation when we interpret η as the probability of detecting a photon, and, conversely, $1-\eta$ is the probability of not detecting a photon. For the case of destructive photon counting, we have

$$\Gamma_\eta(m) = \sum_{k=m}^{\infty}\left[\begin{bmatrix} k \\ m \end{bmatrix}\eta^m(1-\eta)^{k-m}\right]^{1/2}|k-m\rangle_b\langle k| . \tag{4.6}$$

Again for $\eta=1$, we see that $\Gamma\to|0\rangle_b\langle m|$, the expected projection operator.

The probability of obtaining the result $\hat{\rho}^m$ for the conditioned system is given in terms of the effect $\hat{F}_\eta(m)$, where

$$P_\eta(m) = \text{tr}_{abc}[\hat{\rho}\hat{F}_\eta(m)] \tag{4.7}$$

and

$$\hat{F}_\eta(m) = \hat{\Gamma}_\eta^\dagger(m)\Gamma_\eta(m) = \sum_{k=m}^{\infty}\begin{bmatrix} k \\ m \end{bmatrix}\eta^m(1-\eta)^{k-m}|k\rangle_b\langle k| . \tag{4.8}$$

The effect $\hat{F}_\eta(m)$ does not depend on whether the measurement of $\hat{n}_b$ was destructive or not. To calculate $P_\eta(m)$, we do not care about the final state of the b mode and trace over all modes. However, the conditioned density matrix $\hat{\rho}^m$ in Eq. (4.4) is very dependent on the form of the operation.

For the time being, we restrict our attention to the case of $\eta=1$, and the probability to detect m photons in mode b is

$$P_1(m) = \text{tr}_{abc}(|m\rangle_b\langle m|\psi_{\text{out}}\rangle\langle\psi_{\text{out}}|) = \int_{-\infty}^{\infty} dx\,|C_m(\kappa x)|^2|\langle x|\phi_c\rangle|^2 . \tag{4.9}$$

The rotation matrix factors $|C_m(\kappa x)|^2$ act as an envelope for the $\hat{X}_c$ probability distribution of the input state, $|\langle x|\phi_c\rangle|^2$.

As an example, we consider the signal input state to have a Gaussian wave function of the form

$$\langle x|\phi_c\rangle = (2\pi\Delta_c)^{-1/4}e^{-(x-\alpha)^2/4\Delta_c} , \tag{4.10}$$

where α and Δ_c are the mean and variance, respectively, of $\hat{X}_c$. The resulting photon count probability for α real is

$$P_1(m)=\begin{bmatrix}N\\m\end{bmatrix}2^{-2N}(-1)^m\sum_{k=0}^{2(N-m)}\sum_{l=0}^{2m}\begin{bmatrix}2(N-m)\\k\end{bmatrix}\begin{bmatrix}2m\\l\end{bmatrix}(-1)^l\cos[\kappa\alpha(N-k-l)]\exp\left[-\frac{\kappa^2\Delta_c}{2}(N-k-l)^2\right]. \quad (4.11)$$

It is of interest to note that this probability distribution is cyclic in α, the real coherent-state displacement, and is unchanged for $\alpha'=\alpha\pm(2n\pi/\kappa)$ for integral n. This is a direct consequence of the amplitude envelope $|C_m(\kappa x)|^2$ being fully periodic for all values of x. The probe photon-number distribution depends on the relative positioning of the input probability amplitude $|\langle x|\phi_c\rangle|^2$ and the amplitude envelope $|C_m(\kappa x)|^2$ and not on the absolute value of α. (Of course, the signal-mode photon-number distribution is very different for different α.)

In Fig. 2 we plot $P_1(m)$ versus m for $N=15$, $\alpha=0$, and $\Delta_c=1.0$ for various values of κ. This gives some insight into the physical processes at work. There are three regimes of physical interest in this distribution. When $\kappa=0$, the interaction is turned off, and naturally $P_1(m)=\delta_{m0}$. The next regime is with $\kappa\ll 1$ where we see that there is a decaying probability of observing a large photon count in the b mode. This is the regime in which all possible experiments will operate. Finally, we see that if κ is sufficiently strong, then the only contributions to the double sum in Eq. (4.11) will come from terms where $N=k+l$. The contributions to this sum will maximize for values of m of either $m\approx 0$ or $m\approx N$. This can be seen in Fig. 2, where for large κ, the photon count probability distribution is symmetric about a minimum at $m\approx N/2$.

Physically, the distributions for $\kappa\ll 1$ and $\kappa\gg 1$ can be understood by considering in more detail the unitary evolution operator

$$\begin{aligned}U&=e^{-i\kappa\hat{X}_c\hat{J}_x}\\&=\int_{-\infty}^{\infty}dx\,|x\rangle\langle x|e^{-i\kappa x\hat{J}_x}\\&=\int_{-\infty}^{\infty}dx\,|x\rangle\langle x|e^{iq(ab^\dagger+a^\dagger b)},\end{aligned} \quad (4.12)$$

where $q=(\kappa x)/2$. As mentioned above, the unitary evolution of this system can be considered as a rotation in angular momentum space, or, alternatively, as a two-mode mixing operator.[22] In either case the physical interpretation of these operators can be easily understood when the signal mode is prepared in some near eigenstate of $\hat{X}_c$. In this case there will be only one contribution to the integral in Eq. (4.12), and the output state $|\psi_{\text{out}}\rangle$ will show all the features of a unitarily mixed two-mode state. This includes the usual cyclic projection of the two-mode probe from the state $|N,0\rangle$ at "times" $q=n\pi$ $(n=0,1,2,\ldots)$, to the state $|0,N\rangle$ at "times" $q=(n\pi/2)$ $(n=1,3,5,\ldots)$. When the signal mode is not prepared in some near eigenstate of $\hat{X}_c$, then the integral in Eq. (4.12) will generate a weighted average of all possible rotations or mixing of the two-mode probe state. For $\kappa\ll 1$, and for a squeezed vacuum input, the amplitude of the contribution at $q=\pi/2$ (in the state $|0,N\rangle$) will be neglible and we see the decaying probability seen in Fig. 2. However, for $\kappa\gg 1$, there will be many sizable contributions from both of the states $|N,0\rangle$ and $|0,N\rangle$, as well as all other possible states that maintain the total photon number. However, the probability amplitude of all these contributing states will be of order unity only for the above two states. The contributions to the probability amplitudes for the other states will be small for large N. We then see a double-winged probability distribution as depicted in Fig. 2.

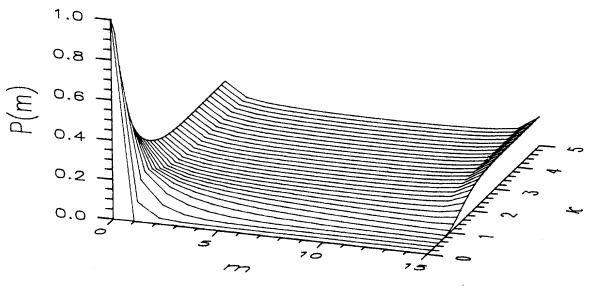

FIG. 2. The photon-number probability distribution for the conditioning measurement of the b mode. The signal mode is prepared in a phase squeezed state. The strength of the parametric interaction is given by κ. The total number of probe photons is $N=15$. These values of κ and N are chosen to demonstrate the ranges $N\kappa^2\ll 1$ and $N\kappa^2\gg 1$.

The conditioned density matrix for the c mode given m readout photons, unit quantum efficiency, and destructive photon counting is

$$\begin{aligned}\hat{\rho}_c^m&=\text{tr}_{ab}(|m\rangle_b\langle m|\psi_{\text{out}}\rangle\langle\psi_{\text{out}}|)/P_1(m)\\&=|\Phi\rangle\langle\Phi|,\end{aligned} \quad (4.13)$$

where the state of the conditioned signal mode is

$$|\Phi\rangle=[P_1(m)]^{-1/2}\int_{-\infty}^{\infty}dx\,C_m(\kappa x)\langle x|\phi_c\rangle|x\rangle. \quad (4.14)$$

The resulting c-mode probability distribution for the $\hat{X}_c$ quadrature component (with value x) is

$$P^m(x)=[P_1(m)]^{-1}|C_m(\kappa x)|^2|\langle x|\phi_c\rangle|^2. \quad (4.15)$$

The rotation matrix factor $|C_m(\kappa x)|^2$ acts as an amplitude envelope for the (generally) Gaussian input probability distribution $|\langle x|\phi_c\rangle|^2$. For large N, $|C_m(\kappa x)|^2$ can be a very sharply peaked function of x. The peaks of this function occur for values of x satisfying $\cos(\kappa x)=(N-2m)/N$ exactly as required from our previous heuristic analysis.

As an example, we compute the conditional distribution in Eq. (4.15) for the Gaussian state [Eq. (4.10)]. In the case $\alpha=0$ and $\Delta_c<\frac{1}{4}$, this is a squeezed vacuum state with reduced fluctuations in $\hat{X}_c$. In the region $x\approx 0$ and

for large N, $|C_0(\kappa x)|^2$ is a sharply peaked function of half width $\Delta \approx (8/\kappa^2 N)^{1/2}$ (for small κ). The input distribution [Eq. (4.10)] has half width $\Delta_i = [8\Delta_c \ln(2)]^{1/2}$. For cases where $\Delta < \Delta_i$, we expect the signal mode to be further squeezed. Typically achievable values of κ are very small (e.g., $\kappa = \chi t \sim 10^{-8}$) and so we are interested in regimes with N very large (e.g., $N \geq 10^{16}$). The systems envisaged use a second-order nonlinearity $\chi \approx 50-500$ s^{-1} (e.g., for KDP) (Ref. 26) and an interaction time of the order of 10^{-11} s. If we consider a classical coherent pump state in the mode with $|\alpha|^2 \approx N \approx 10^{16}$, we achieve a typical interaction strength of $\alpha\chi t \approx 0.5$.

The $|C_m(\kappa x)|^2$ envelope is multivalued and has side peaks at values [given by Eq. (2.20)] of $x \approx n\pi/\kappa$, for $N \gg m$, and $n = 0,2,4,\ldots$. For small κ these peaks are widely separated and for squeezed input states (with narrow $\hat{X}_c$ probability distributions), we expect very low amplitude for the sideband superposition peaks. Conversely, for very broad input x distributions (for example, states in which $\hat{Y}_c$ is squeezed), then the conditioned signal mode would be in a superposition of amplitude squeezed states.

That this is so can be seen in plots of the conditioned probability distributions for the $\hat{X}_c$ quadratuare of the signal mode. These conditions are illustrated in Figs. 3–5, where we again use the analogous regime of $N = 15$ and $0 \leq \kappa \leq 5$. In Fig. 3 we show the case when the measured b-mode photon count is zero ($m = 0$). The signal-mode input state $\hat{X}_c$ distribution is shown at the point $\kappa = 0$ (the interaction is turned off). The input signal state is a squeezed vacuum with $\Delta_c > \frac{1}{4}$. The values of N, m, κ, and Δ_c are chosen to illustrate features of the probability distributions, and are just indicative of the distributions obtained using more physically reasonable parameters.

The two dominant features of the distribution in Fig. 3 (and subsequent figures) are the enhanced squeezing for strong κ in all the peaks and the multiple side peaks which lie on values of x satisfying $\cos(\kappa x) = (N - 2m)/N$. In addition, each of these side peaks together with the central peak undergoes a further splitting for $m > 0$. This is reminiscent of the superpositions of macroscopic coherent states displayed in Ref. 5, where classical pumping was employed, and occurs for a similar reason. In Ref. 5, Song and Caves showed that this superposition of states results from a measurement of $\hat{X}_c^2$, and, therefore, the conditioned $\hat{X}_c$ distribution will center on positive and negative values. Our measurement of $\hat{n}_b$ for small κ is equivalent to a measurement of $\hat{X}_c^2$, and we expect a similar repeated double-peak structure. The new feature is the presence of many sideband superpositions. The conditioned signal mode is in a superposition of many squeezed states. (Note that for $m > 0$ in Fig. 4 there is zero probability of obtaining a photon count of $m > 0$ for an interaction strength of $\kappa = 0$. Hence, the $\kappa = 0$ line in these figures is always equal to zero.)

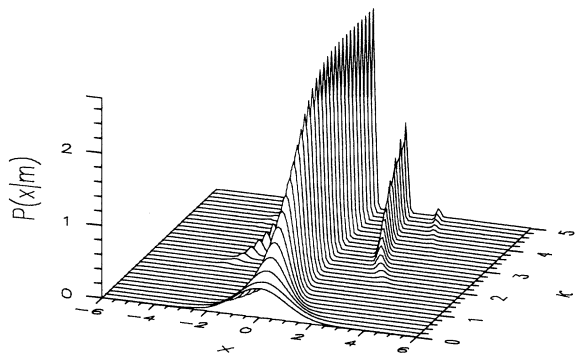

FIG. 3. The conditioned probability distribution for the signal-mode quadrature $\hat{X}_c$. The signal mode is prepared in a squeezed state with $V(X_c) > \frac{1}{4}$ (seen when $\kappa = 0$). The strength of the parametric interaction (κ) and the total probe photon number ($N = 15$) are chosen to be illustrative. (Here, $M = 0$ photons are measured in the b mode.) Note the enhanced squeezing of the distributions for strong κ, and the presence of the side peaks showing the expected superposition of squeezed states.

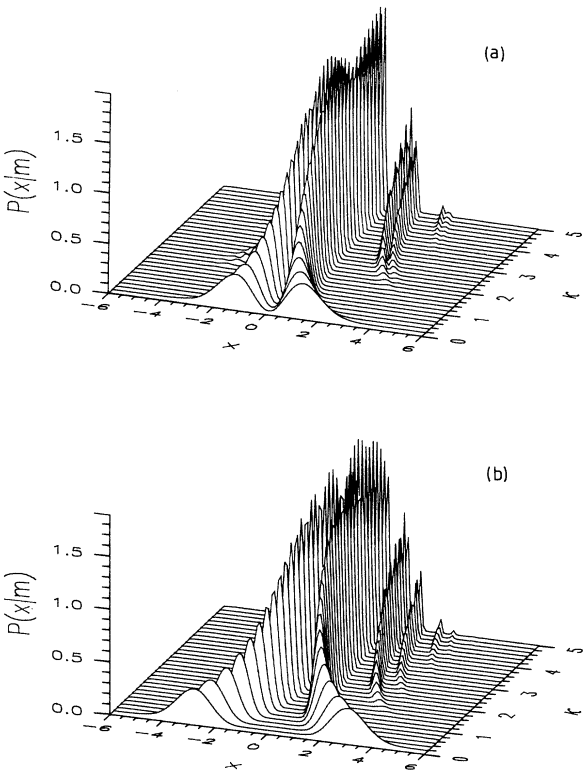

FIG. 4. The conditioned probability distribution for the signal-mode quadrature $\hat{X}_c$ given a measurement of (a) $m = 1$ and (b) $m = 5$ photons in the b mode of the probe. The strength of the parametric interaction (κ) and the total photon number ($N = 15$) are chosen to be illustrative. The new feature is the presence of double peaks for $m \neq 0$. This results from the double-valued nature of a measurement of $\langle \hat{X}_c^2 \rangle$. In (b) with $m = 5$, we see the peaks separating as expected for increasing m. The peaks lie at points satisfying $\cos(\kappa x) = (N - m)/m$.

V. NONUNIT QUANTUM DETECTOR EFFICIENCY

It is well known that even small levels of inefficiency in the photodetector will wash out interference[27] and coherence effects.[5] The system being considered here offers the intriguing possibility that the noise introduced by nonunit quantum efficiency can be partially overcome. This results from the fully quantized treatment of the pump mode which has been prepared in a number state with very large photon-number occupancy ($N \gg 1$). It turns out that the inefficiencies in photon detection occur only in terms proportional to N^{-1}. Hence, for large N, the effect of the detector inefficiencies is reduced.

This possibility of mitigating the effects of nonunit quantum detector efficiency ($\eta < 1$) by using the reduced-noise properties of a number state pump suggests we first discuss the effects of using generalized pump-mode states such as might be produced using the feedback mechanisms of Fig. 1. These states have reduced photon fluctuations below that of coherent pump states, $0 \le V(\hat{n}_a) \le \langle \hat{n}_a \rangle$. We introduce a generalized a-mode pump state of

$$\hat{\rho}_a^{\text{in}} = (2\pi\lambda N)^{-1/2} \sum_{k=0}^{\infty} e^{[-(k-N)^2]/(2\lambda N)} |k\rangle_a \langle k| \ . \tag{5.1}$$

This state has mean photon number of N and $V(\hat{n}_a) = \lambda N$. We see that a variation in λ over the range [0,1] gives the desired range of reduction in the photon fluctuation. Indeed, we see that for $\lambda = 0$, the exponential in Eq. (5.1) approximates a δ function and $\rho_a^{\text{in}} = |N\rangle\langle N|$. For $\lambda = 1$, and noting for $N \gg 1$ that the photon-number distribution is very narrowly peaked about the mean value of N, the input pump state approximates that of a diagonalized coherent state. The advantage of using this pump-mode input state is that for $N \gg 1$, we can closely approximate the sums over k by integrals over the same range. The effectiveness of this approximation is checked by comparison to exact calculations later in this section.

We include the effects of nonunit quantum detector efficiency ($\eta < 1$) by the well-known procedure of interposing a beam splitter of transmittivity $\sqrt{\eta}$ between the system and a perfect photodetector. The desired SNR as defined in Eq. (3.1) is then

$$\mathcal{S}_{\eta,\lambda} = \frac{1 - \langle \hat{O}_c \rangle}{\left[V(\hat{O}_c) + \frac{\lambda - 1}{N} \langle \hat{O}_c^2 \rangle - \frac{2(\lambda\eta + 1 - \eta)}{N\eta} \langle \hat{O}_c^{\,2} \rangle + \frac{\eta(1+\lambda) + 2(1-\eta)}{N\eta} \right]^{1/2}} \ , \tag{5.2}$$

where $\hat{O}_c = \cos(\kappa \hat{X}_c)$ and $V(\hat{O}_c)$ is the variance of $\hat{O}_c$. We see here that for $\lambda = 0$ and $\eta = 1$ we reproduce Eq. (3.2) for the photon-number state pump. For $\lambda = 0$ but $\eta < 1$ we see that for large N, all the terms involving η in the denominator do not contribute (for $\eta > 0$), and in this regime for $0 < \eta < 1$, $\mathcal{S}_{\eta,0}$ is independent of η.

Expanding the $\cos(\kappa \hat{X}_c)$ terms in the above equation (for $\kappa \ll 1$) gives insight into the relative importance of the sizes of N, κ, η, and λ. We have

$$\mathcal{S}_{\eta,\lambda} = \frac{\langle \hat{X}_c^{\,2} \rangle}{\left[V(\hat{X}_c^{\,2}) + \frac{2\eta\lambda - 2\eta - 1}{3N\eta} \langle \hat{X}_c^{\,4} \rangle + \frac{4}{N\eta\kappa^2} \langle \hat{X}_c^{\,2} \rangle \right]^{1/2}} . \tag{5.3}$$

Evidently, the effects of inefficiency in the photon detection process can be mitigated when $N\kappa^2\eta \gg 4$ and $3N\eta \gg 2\eta\lambda - 2\eta - 1$. For $\lambda \in [0,1]$ we see that the first condition is sufficient to eliminate the dependence of $\mathcal{S}_{\eta,\lambda}$ on the photon detector inefficiency. For $\eta \in [0,1]$ the second condition breaks down only for values of $\lambda \sim \frac{3}{2}N$. This corresponds to the input pump state having a photon-number variance of $V(\hat{n}_a) \sim \frac{3}{2}N^2$, which is very broad. This result justifies in part the observability of the results obtained in Ref. 5 where a classical nondepleted coherent-state pump was used in a detection scheme based on $\langle \hat{X}_c^{\,2} \rangle$ as above. For $\eta \to 0$, we have that $\mathcal{S}_{0,\lambda} \to 0$ as expected.

We can perform exact calculations for the pump mode prepared in a number state and for certain generalized mixed states. We are also interested in the probability distribution for the signal-mode $\hat{X}_c$ quadrature given $\eta < 1$.

From Eq. (4.7), with nonunit quantum efficiency $\eta < 1$, and for either a QND or destructive photon measurement, we have the observed photon-count distribution of

$$P_\eta(m) = \sum_{k=m}^{\infty} P_1(k) \binom{k}{m} (1-\eta)^{k-m} \eta^m \ , \tag{5.4}$$

where $P_1(k)$ is the calculated photon distribution in Eq. (4.9). The probability distribution of the signal-mode $\hat{X}_c$ quadrature (with eigenvalue x) can be calculated from the conditioned three-mode density matrix $\hat{\rho}^m$ [Eq. (4.4)] with number state pump giving

$$\begin{aligned} P_\eta^m(x) &= \mathrm{tr}_{ab}(|x\rangle_c \langle x| \hat{\rho}^m)/P_\eta(m) \\ &= P_\eta^{-1}(m) \binom{N}{m} \eta^m \bar{s}^{\,2m} (1 - \eta\bar{s}^{\,2})^{N-m} |\langle x|\phi_c\rangle|^2 \ , \end{aligned} \tag{5.5}$$

where $\bar{s} = \sin(\kappa x/2)$. In the limit as $\eta \to 1$, Eq. (5.5) reduces to Eq. (4.15) as expected.

The nonunit quantum efficiency (η) only appears twice in this equation. The first appearance is a nonessential amplitude factor. The effect of the second η can be more than compensated for by making N large for small κ as suggested by the signal-to-noise ratio for $\eta<1$. This ratio depends, as usual, on the averages of various powers of the measurement variable $\hat{n}_b$. That is,

$$\langle \hat{n}_b^{\alpha} \rangle = \sum_{m=0}^{\infty} m^{\alpha} P_{\eta}(m) \ . \tag{5.6}$$

An exact calculation of the SNR for a number-state input duplicates the results of Eq. (5.2).

We show examples of the conditioned $\hat{X}_c$ probability distribution for $\eta<1$ in Fig. 5 (with number-state pump). Using the analogous values of $N=15$, $0\le\kappa\le 5$ in Fig. 5(a), with $\eta=0.5$, we see that there is very little loss of definition. In Fig. 5(b) with $\eta=0.1$, we begin to see a loss of features. This regime has $N\kappa^2\eta\approx 6$ for $\kappa=2$. In the physically reasonable regimes with $N\sim 10^{16}$, $\kappa\sim 10^{-8}$, then the beneficial noise properties of a number-state pump might offer a means to allow for the effects of the nonunit quantum efficiency of photon detection.

The cause of this mitigation in the effects of detector inefficiencies is the reduced-pump-noise properties when we prepare the pump in a number state. It is of interet to calculate exactly the effects of preparing the pump mode in a mixture of number states. We set the initial pump-mode density matrix as

$$\hat{\rho}_{\rm in}^{a} = \sum_{k=0}^{\infty} P_k^a |k\rangle_a\langle k| \ . \tag{5.7}$$

All the previous derivations follow routinely, including contributions from the initial mixture of states in the pump probe. In particular, for unit quantum efficiency ($\eta=1$), we have a probability distribution for counting m photons in the b mode [see Eq. (4.9)]:

$$\begin{aligned} P_1(m) &= \sum_{k=0}^{\infty} P_k^a \mathrm{tr}_{abc}(|m\rangle_b\langle m|\rho_{\rm out}^k) \\ &= \int_{-\infty}^{\infty} dx\, |C_m'(\kappa x)|^2 |\langle x|\phi_c\rangle|^2 \ . \end{aligned} \tag{5.8}$$

The form of this equation is identical to that of Eq. (4.9). The only difference is the redefined matrix elements

$$|C_m'(\kappa x)|^2 = \left[\frac{\bar{s}}{\bar{c}}\right]^{2m} \sum_{k=m}^{\infty} \begin{bmatrix} k \\ m \end{bmatrix} P_k^a \bar{c}^{\,2k} \ , \tag{5.9}$$

where $\bar{s}=\sin(\kappa x/2)$ and $\bar{c}=\cos(\kappa x/2)$.

Here, it is seen that the only possible contributions to a measurement of m photons in the b state come from only those pump-mode states with at least m photons in them. In the case where $P_k^a=\delta_{kN}$, then the previous rotation matrix elements in Eq. (4.3) are obtained. The form of all our previous results is unchanged except that we now use these modified rotation matrices.

A particular example is to take a normalized and Poisson input number-state distribution in the a mode. Here we set

$$P_k^a = e^{-|\alpha|^2}\frac{|\alpha|^{2k}}{k!} \tag{5.10}$$

for some $|\alpha|^2=N$. This pump state is roughly equivalent to that of Eq. (5.1) in the limit $\lambda=1$, $N=|\alpha|^2\gg 1$. Then we see that

$$|C_m'(\kappa x)|^2 = \frac{1}{m!}(|\alpha|\bar{s})^{2m} e^{-(|\alpha|\bar{s})^2} \ , \tag{5.11}$$

where $\bar{s}=\sin(\kappa x/2)$. The exponential in these rotation matrices is interesting in that it is guaranteed to be equal to one whenever $\bar{s}=0$ and this occurs periodically along the x axis. For points where $\bar{s}\neq 0$, and with $|\alpha|^2$ a large number, then the rotation matrix elements will tend to zero. And it is these elements which serve as an amplitude envelope for the input $|\langle x|\phi_c\rangle|^2$ distribution. Superpositions of states will still occur but they will be widely spaced and extremely narrow—that is, highly squeezed.

Throughout this paper we have been relating results obtained for a number-state pump with those of the classical nondepleted pump. The results of Eq. (5.11) are intermediate between using a number-state pump and using a coherent-state pump. A classical nondepleted pump is different again in that it is restricted from evolving under

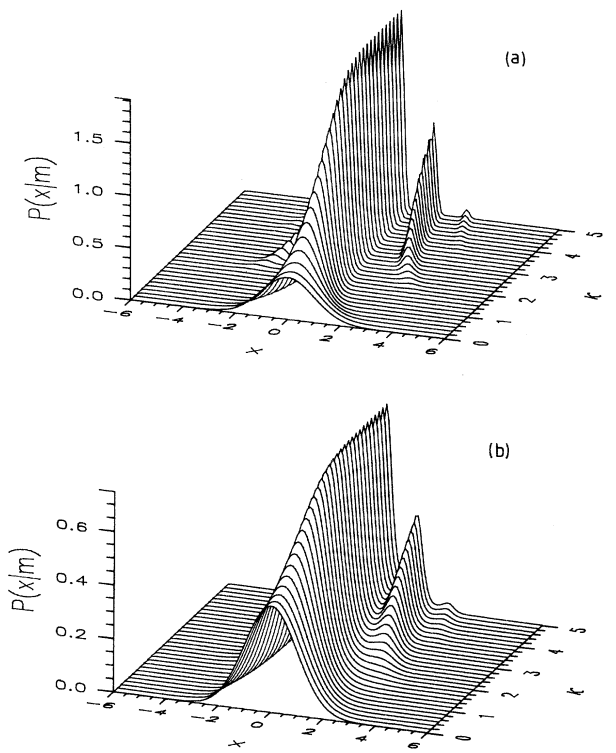

FIG. 5. The conditioned probability distribution for the signal-mode quadrature $\hat{X}_c$ with a nonunit quantum efficiency ($\eta<1$). The strength of the parametric (κ) and the total probe photon number are chosen to be illustrative. In (a) we show $\eta=0.5$. There is practically no loss of definition in the features compared to Fig. 1. Only in (b), with $\eta=0.1$, do we begin to see a smearing of the peaks. This illustrates that the effects of η can be mitigated if $N\kappa^2\eta\gg 1$.

the interaction Hamiltonian. For an input probe state of $|\alpha,0\rangle_{a,b}$, the interaction Hamiltonian acts like a two-mode mixer.[22] In this case the unitarily evolved output state is

$$|\psi_{\text{out}}\rangle = \int dx \langle x|\phi_c\rangle |\alpha_1,\alpha_2,x\rangle \ , \tag{5.12}$$

where $\alpha_1=\alpha\cos(\kappa x/2)$ and $\alpha_2=-i\alpha\sin(\kappa x/2)$. The probability distribution of $\hat{X}_c$, given m measured photons in the b mode and unit quantum efficiency, is

$$P^m(x)=[P(m)]^{-1}|\langle x|\phi_c\rangle|^2\frac{1}{m!}(|\alpha|\bar{s})^{2m}e^{-(|\alpha|\bar{s})^2} \ . \tag{5.13}$$

Song and Caves in Ref. 5 demonstrated a superposition of two coherent states. This result can be seen in Eq. (5.13) where we see the amplitude envelope for $|\langle x|\phi_c\rangle|^2$ is double peaked in the range $x\approx 0$, and side peaks are widely separated and of very low amplitude.

VI. CONCLUSION

In this paper we fully quantized the three-mode parametric interaction and considered the beneficial effects of pumping this system with a number state. This allows us to treat the system-probe interaction as rotations of the angular momentum vector of the probe system. The degree of rotation depends on the input distribution of the signal-mode quadrature of interest. With this model in mind, we can clearly see that any particular probe state (specified by a direction in angular momentum space) is generated by many particular values of the signal-mode quadrature. We do a conditioning measurement on the probe to locate this probe-state vector and condition the signal-mode quadrature probability distribution. This will peak at those values which generate (by rotation) the measured probe state. This conditioning measurement is equivalent to simple photon counting. Then the signal is conditionally projected into a superposition of near eigenstates of the quadrature of interest. These results are similar to those obtained using a classical pump.

There are some beneficial noise effects obtained by using a number-state pump. We show this by an analysis of the signal-to-noise ratio achieved by this system. In certain regimes, our system gives better results than can be achieved by balanced homodyne detection. We give a simple interpretation of these results in terms of higher-order squeezing. Our conditioning measurement is shown to be equivalent to a measurement of the noise in the signal quadrature of interest. This higher-order moment of the signal mode has previously been shown to have enhanced squeezing and hence beneficial signal-to-noise ratios.

Finally, we show that using a number-state pump offers intriguing possibilities in countering the effects of nonunit quantum photon detection efficiency. For large number-state occupancy of the pump mode we show that the signal-to-noise ratio can be independent of the photon detection efficiency. These results also apply for more general pump states with reduced photon-number fluctuation.

[1] A. La Porta, R. E. Slusher, and B. Yurke, Phys. Rev. Lett. **62**, 28 (1989).

[2] B. Yurke, J. Opt. Soc. Am. B **2**, 732 (1985).

[3] H. A. Bachor, M. D. Levenson, D. F. Walls, S. H. Perlmutter, and R. M. Shelby, Phys. Rev. A **38**, 180 (1988).

[4] S. Song, C. M. Caves, and B. Yurke, Phys. Rev. A **41**, 5261 (1990).

[5] M. D. Levenson, R. M. Shelby, M. Reid, and D. F. Walls, Phys. Rev. Lett. **57**, 2473 (1986).

[6] B. Yurke and D. Stoler, Phys. Rev. Lett. **57**, 13 (1986).

[7] G. J. Milburn, Phys. Rev. A **33**, 674 (1986).

[8] G. J. Milburn and C. A. Holmes, Phys. Rev. Lett. **56**, 2237 (1986).

[9] B. Yurke, S. L. McCall, and J. R. Kaluder, Phys. Rev. A **33**, 4033 (1986).

[10] B. C. Sanders, Phys. Rev. A **40**, 2417 (1989).

[11] J. Schwinger, U.S. Atomic Energy Commission Report No. NYO-3071 (U.S. GPO, Washington, D.C., 1952), reprinted in *Quantum Theory of Angular Momentum,* edited by L. C. Biedenharn and H. van Dam (Academic, New York, 1965).

[12] Y. Yamamoto and S. Machida, Phys. Rev. A **34**, 4025 (1986).

[13] S. Machida and Y. Yamamoto, Opt. Commun. **57**, 290 (1986).

[14] J. H. Shapiro, G. Saplakoglu, S.-T. Ho, P. Kumar, B. E. A. Saleh, and M. C. Teich, J. Opt. Soc. Am. B **4**, 1604 (1987).

[15] G. J. Milburn, in Proceedings of Gravitational Astronomy—Instrument Design and Astrophysical Prospects, edited by D. McClleland (World Scientific, Singapore, in press).

[16] G. J. Milburn and D. F. Walls, Phys. Rev. A **28**, 2065 (1983).

[17] B. L. Schumaker, Opt. Lett. **9**, 189 (1984).

[18] C. C. Gerry and P. J. Moyer, Phys. Rev. A **38**, 5665 (1988).

[19] C. K. Hong and L. Mandel, Phys. Rev. Lett. **54**, 323 (1985).

[20] M. J. Holland, M. J. Collett, D. F. Walls, and M. D. Levenson, Phys. Rev. A **42**, 2995 (1990).

[21] J. M. Norman, *A Lie Group: Rotations in Quantum Mechanics* (North-Holland, Amsterdam, 1980).

[22] B. L. Schumaker, Phys. Rep. **135**, 318 (1986).

[23] K. Kraus, *States, Effects and Operations: Fundamental Notions of Quantum Theory* (Springer-Verlag, Berlin, 1983).

[24] C. M. Caves, Phys. Rev. D **33**, 1643 (1986); **35**, 1815 (1987).

[25] G. J. Milburn, Phys. Rev. A **36**, 5271 (1987).

[26] P. D. Drummond, K. J. McNeil, and D. F. Walls, Opt. Acta **27**, 321 (1980).